

Anomalously thick domain walls in ferroelectrics

P. V. Yudin,^{1,*} M. Y. Gureev,¹ T. Sluka,^{1,2} A. K. Tagantsev,¹ and N. Setter¹

¹*Ceramics Laboratory, Swiss Federal Institute of Technology (EPFL), CH-1015 Lausanne, Switzerland*

²*DPMC-MaNEP, University of Geneva, 24 Quai Ernest Ansermet, 1211 Geneva 4, Switzerland*

(Received 30 August 2013; revised manuscript received 22 January 2015; published 18 February 2015; corrected 20 February 2015)

Using the Landau theory we demonstrate the possibility of unusual, anomalously thick ferroelectric domain walls, where the order parameter rotates with a nearly constant modulus as in ferromagnets. The effect occurs in 90° charged domain walls and is associated with the easy polarization rotation near the morphotropic phase boundary. This magneticlike profile is unique to charged domain walls due to the availability of free charges which screen the depolarizing field resulting from polarization rotation. In contrast to previously known thick ferroelectric domain walls, the large thickness of 90° charged domain walls near the morphotropic boundary is predicted for a wide temperature interval. This property may be favorable for potential applications.

DOI: [10.1103/PhysRevB.91.060102](https://doi.org/10.1103/PhysRevB.91.060102)

PACS number(s): 77.80.Dj, 72.20.Jv

Ferroelectric domain walls (DWs) are nanometric-scale transitions between two domain states which differ in the orientation of a switchable spontaneous polarization. Unlike in ferromagnets, where DWs are typically 100 nm thick and magnetization rotates with a nearly constant modulus [1], DWs in ferroelectrics are typically extremely thin, mostly <2 nm, and polarization reduces its modulus in the DW region [2]. Because of their small thickness, ferroelectric DWs have been often regarded as boundaries without significant intrinsic functionality. The recent progress in experimental and computational techniques has led to discoveries of intriguing phenomena such as the photovoltaic effect [3] and conductivity [4] located at ferroelectric DWs. Furthermore, bistable DWs with a switchable intrinsic chirality of polarization have been theoretically predicted [5], hence promising the intrinsic memory capabilities of DWs. In view of these discoveries, the fundamental research of the internal structure of ferroelectric DWs has gained interest.

In the present Rapid Communication we demonstrate the possibility of unusual ferroelectric DWs where the order parameter behaves as in ferromagnets, resulting in anomalously thick DWs. Such a situation occurs in 90° charged domain walls (CDWs) in morphotropic phase boundary (MPB) systems.

CDWs are domain walls with electrically incompatible orientations $\Delta \vec{P} \cdot \vec{n} \neq 0$, where \vec{n} is DW normal, and $\Delta \vec{P}$ is the polarization jump between the domain states. If the compatibility condition is met, the DW is electrically neutral. In CDWs bound charge $\rho_b = -\text{div } \vec{P}$ is accumulated within the CDW region. In typical perovskite ferroelectrics, only CDWs with orientations that are slightly incompatible may withstand the depolarizing field produced by their own polarization charges [6], otherwise screening by free carriers is needed. In this Rapid Communication we address so-called strongly charged DWs [7]. Such walls create a depolarizing field which, if not screened by free carriers, would destabilize the ferroelectricity in the adjacent domains. In perovskite ferroelectrics, strongly CDWs occur once the polarization jump at the wall is of the order of spontaneous polarization ($\Delta P \simeq P_0$). According to estimates [8,9], the existence of strongly CDWs in per-

ovskite ferroelectrics requires almost perfect compensation of the bound charge by free charges, $\rho_f \simeq -\rho_b$. The charge compensation can be provided by mobile defects [10,11] or by free electrons or holes. In the latter case, CDWs may exhibit intriguing electronic properties [8,9]. Of particular interest for potential applications is their giant metallic-type conductivity, in sharp contrast to the insulating bulk [7].

Currently, a Landau theory description is available only for 180° CDWs [9]. The theory demonstrates that, in typical ferroelectric perovskites, 180° CDWs are expected to be about one order of magnitude thicker than neutral DWs, which is in agreement with the reported transmission electron microscopy (TEM) observation of 180° CDWs in $\text{Pb}(\text{Zr},\text{Ti})\text{O}_3$, having a thickness of $\simeq 7$ nm [12]. Thick DWs are attractive objects for fundamental studies as they may allow a detailed insight into their internal structure. Additionally, thick CDWs with pronounced intrinsic properties can control the macroscopic behavior of ferroelectrics.

The present research is inspired by recent discoveries linked with 90° CDW patterns in prototypical ferroelectric BaTiO_3 [7,13]. Numerical simulations indicated that 90° CDWs may be still thicker than 180° CDWs [13]. Unlike 180° CDWs, 90° CDWs are also ferroelastic, which makes them more robust and industrially promising. First, 90° CDWs are stabilized by mechanical clamping and, second, domains separated by 90° CDWs have a common component of polarization. These two factors can be profitably used to control the formation of CDWs and to manipulate with them.

In this Rapid Communication we provide a Landau theory of strongly charged 90° domain walls for the situation where the bound charge of the wall is virtually completely screened by the electronic free charge, a situation typical for perovskite ferroelectrics. The theory identifies the origin of the anomalous CDW thickness to be related to the large anisotropy of the dielectric susceptibility. Such anisotropy arises in ferroelectrics near the phase transition between two different ferroelectric phases. In BaTiO_3 it occurs at room temperature [14], where the material is close to a temperature-driven transition from the tetragonal to the orthorhombic phase. Such a situation also takes place near the morphotropic phase boundary (MPB) in perovskite solid solutions with tetragonal-rhombohedral composition-driven phase transitions. A classical example is lead zirconate titanate (PZT) where the morphotropic-

*petr.yudin@epfl.ch

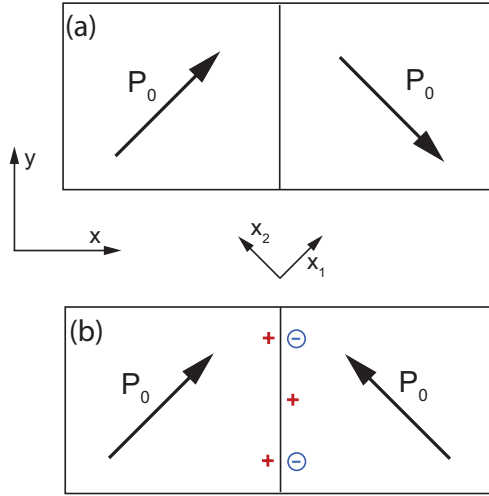


FIG. 1. (Color online) Scheme of mechanically compatible 90° domain walls: (a) electrically neutral and (b) charged. P_0 is the spontaneous polarization in the domains.

boundary compositions are of high practical interest in view of their enhanced electromechanical properties.

The possibility of CDW widening near the MPB can be elucidated in terms of a simple Landau model which neglects electromechanical coupling. Let us consider a perovskite ferroelectric with a second-order phase transition on the tetragonal side of the MPB between the tetragonal and rhombohedral phases. We cut a {110}-oriented parallel plate out of this material, construct a capacitor, and short-circuit the electrodes.

There are two types of mechanically compatible 90° DWs possible inside such a capacitor: neutral, shown in Fig. 1(a), and charged, shown in Fig. 1(b) [15]. The system is described by the equations of state for the electric polarization, which have the form (see, e.g., Ref. [16])

$$E_1 = \alpha P_1 + \beta_1 P_1^3 + \beta_2 P_1 P_2^2 - g_{11} \frac{\partial^2 P_1}{\partial x_1^2} - g_{44} \frac{\partial^2 P_1}{\partial x_2^2} - g_{12} \frac{\partial^2 P_2}{\partial x_1 \partial x_2}, \quad (1)$$

$$E_2 = \alpha P_2 + \beta_1 P_2^3 + \beta_2 P_2 P_1^2 - g_{11} \frac{\partial^2 P_2}{\partial x_2^2} - g_{44} \frac{\partial^2 P_2}{\partial x_1^2} - g_{12} \frac{\partial^2 P_1}{\partial x_1 \partial x_2}, \quad (2)$$

where x_1 and x_2 are the Cartesian coordinates of the pseudocubic crystallographic reference frame, \vec{E} is the electric field, \vec{P} is the ferroelectric part of polarization, and g_{ij} is the correlation energy tensor (in Voigt notations), and the Poisson equation

$$\text{div } \vec{D} = \rho_f, \quad (3)$$

where the electrical displacement is defined as

$$\vec{D} = \varepsilon_b \vec{E} + \vec{P}. \quad (4)$$

Here, ε_b is the background dielectric permittivity [17], and ρ_f is the density of free charges. In equilibrium ρ_f is a function

of the electrical potential $\varphi = -\int \vec{E} \cdot d\vec{x}$ only, i.e.,

$$\rho_f = \rho_f(\varphi). \quad (5)$$

We consider the case of electronic screening. The explicit form for Eq. (5) in such a case can be obtained from the consideration of corresponding quantum-mechanical problem (see, e.g., Ref. [9]). Equations (1)–(5) constitute the full set of equations used to determine the polarization distribution in CDW.

In the reference frame of the DW (the x axis is perpendicular and the y axis is parallel to the domain wall plane), the problem allows a one-dimensional (1D) treatment with all the physical quantities depending only on the coordinate x . In this reference frame, Eqs. (1) and (2) can be rewritten as

$$E_x = \alpha P_x + \frac{\beta_1 + \beta_2}{2} P_x^3 + \frac{(3\beta_1 - \beta_2)}{2} P_x P_y^2 - \left(\frac{g_{11} + g_{12}}{2} + g_{44} \right) \frac{d^2 P_x}{dx^2}, \quad (6)$$

$$E_y = \alpha P_y + \frac{\beta_1 + \beta_2}{2} P_y^3 + \frac{(3\beta_1 - \beta_2)}{2} P_y P_x^2 - \left(\frac{g_{11} - g_{12}}{2} \right) \frac{d^2 P_y}{dx^2}. \quad (7)$$

The boundary conditions for the CDW are as follows:

$$P_x|_{-\infty} = P_0/\sqrt{2}, \quad P_x|_{\infty} = -P_0/\sqrt{2}, \quad P_y|_{\pm\infty} = P_0/\sqrt{2}, \quad (8)$$

where $P_0 = \sqrt{-\alpha/\beta_1}$ is the modulus of the spontaneous polarization inside the domains.

From the Poisson equation, Eq. (3), the E_x component of the electric field may be linked with the corresponding polarization component P_x . In the case of strong screening ($\rho_f \simeq -\rho_b$), typical for strongly charged DWs in perovskite ferroelectrics, the approximation $D_x \simeq P_x$ can be used [9] for the electric displacement, Eq. (4). Its substitution to Eq. (3) yields

$$dP_x/dx \simeq \rho_f, \quad (9)$$

which is consistent with $\rho_b = -\text{div } \vec{P}$, in the case where $\rho_f \simeq -\rho_b$. The derivative of Eq. (9) with respect to x using Eq. (5) yields

$$E_x = -\frac{d\varphi}{dx} = -\left(\frac{\partial \rho_f}{\partial \varphi} \right)^{-1} \frac{d^2 P_x}{dx^2}. \quad (10)$$

When substituted into Eq. (6), Eq. (10) determines an additional effective correlation energy term [18]. Gureev *et al.* [9] demonstrated for the case of a 180° CDW that this additional correlation term is—in the case of ordinary perovskite ferroelectrics—typically two orders of magnitude larger than the initial one: $|E_x| \gg g_{ij} \frac{d^2 P_x}{dx^2}$, $ij = 11, 12, 44$. As a consequence, CDWs are a few times thicker than neutral DWs and an approximation can be applied where the initial correlation terms are neglected. We apply this approximation here for a 90° CDW which will be justified *a posteriori* by the fact that they are at least as thick as 180° CDWs. Then Eqs. (6), (7), and (10), and the condition of the short-circuited

sample $E_y = 0$, give

$$\alpha P_x + \frac{\beta_1 + \beta_2}{2} P_x^3 + \frac{(3\beta_1 - \beta_2)}{2} P_x P_y^2 + \left(\frac{\partial \rho}{\partial \varphi}\right)^{-1} \frac{d^2 P_x}{dx^2} = 0, \quad (11)$$

$$\alpha P_y + \frac{\beta_1 + \beta_2}{2} P_y^3 + \frac{(3\beta_1 - \beta_2)}{2} P_y P_x^2 = 0. \quad (12)$$

Eliminating P_y between Eqs. (12) and (11), one obtains

$$\tilde{\alpha} P_x + \tilde{\beta} P_x^3 + \left(\frac{\partial \rho}{\partial \varphi}\right)^{-1} \frac{d^2 P_x}{dx^2} = 0, \quad (13)$$

where

$$\tilde{\alpha} = \alpha \theta, \quad \tilde{\beta} = 2\beta_1 \theta, \quad (14)$$

$$\theta = \frac{2(\beta_2 - \beta_1)}{\beta_2 + \beta_1}. \quad (15)$$

Equation (13) is identical to that found by Gureev *et al.* [9] for the case of a 180° CDW within the substitution

$$\alpha \rightarrow \alpha \theta, \quad \beta_1 \rightarrow 2\beta_1 \theta, \quad P_0 \rightarrow P_0/\sqrt{2}. \quad (16)$$

In Ref. [9] it has been shown that (13) can be solved analytically for a number of limiting cases, where an explicit analytical form for Eq. (5) is available. These cases correspond to the so-called screening regimes where the electronic gas in the wall can be classified as either degenerate or classical and the screening itself as either linear or nonlinear. The CDW half-widths δ_{180} of the polarization profiles obtained in Ref. [9] for these screening regimes can be covered with a generic formula,

$$\delta_{180} = \frac{a}{|\alpha|^b P_0^c}, \quad (17)$$

where $1/2 \leq b \leq 1$ and $0 \leq c \leq 1$, while a is a material-dependent but temperature-independent coefficient. The coefficients a , b , and c depend upon the screening regime.

Applying substitution Eq. (16) to Eq. (17) one readily obtains an expression for the half-widths of 90° CDWs,

$$\delta_{90} = \frac{a 2^{c/2}}{P_0^c |\tilde{\alpha}|^b}. \quad (18)$$

Equation (18) can be rewritten in the form

$$\delta_{90} = \delta_{180} \theta^{-b} 2^{c/2}. \quad (19)$$

The parameter θ from Eq. (15) tends to zero as the morphotropic boundary ($\beta_2 = \beta_1$) is approached, while far away from the MPB it is of the order of unity. This leads to a considerable difference between the widths of the 90° and 180° CDWs near the MPB. The thickness of the 90° CDW, scaling as $|\theta|^{-b}$ ($1/2 \leq b \leq 1$), as controlled by Eq. (19), diverges as one approaches the MPB. At the same time the thickness of the 180° CDW does not undergo considerable changes near the MPB. According to calculations performed in Ref. [9] in perovskite ferroelectrics that are interesting for applications, a so-called nonlinear regime of the bound charge screening takes place, and an approximation may be used where the electron gas

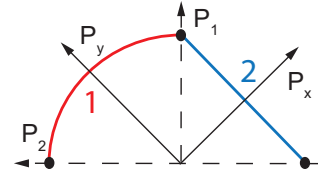


FIG. 2. (Color online) Mapping of the order parameter in the domain walls on the plane $P_1 P_2$. Spontaneous polarization corresponding to the domains is shown as black circles. Approximate trajectories of the order parameter in charged (line 1) and neutral (line 2) 90° domain walls are shown.

becomes degenerate in the CDW region. Using the values of a , b , and c calculated in Ref. [9] for this regime, Eq. (18) yields

$$\delta_{90}^{(ND)} = \left(\frac{9\sqrt{2}\pi^4 \hbar^6}{q^5 m^3 |\alpha \theta|^3 P_0} \right)^{1/5}. \quad (20)$$

Here $\hbar = 1.05 \times 10^{-34}$ J s is the Planck's constant, m is the effective electron mass, and $q = 1.6 \times 10^{-19}$ C is the elementary charge.

The effect of the thickening of 90° CDWs correlates with the anisotropy of the dielectric susceptibility. In the approximation under consideration, expressions for the components of dielectric susceptibility tensor have the form [19]

$$\chi_{\parallel} = \frac{-1}{2\alpha}, \quad \chi_{\perp} = \frac{-\beta_1}{\alpha(\beta_2 - \beta_1)}. \quad (21)$$

Here χ_{\parallel} and χ_{\perp} are susceptibilities in directions parallel to, and perpendicular to, the spontaneous polarization, or longitudinal and transverse susceptibilities, respectively. From Eq. (21) one readily obtains

$$|\alpha| = \frac{1}{2\chi_{\parallel}}, \quad |\tilde{\alpha}| = \frac{1}{\chi_{\parallel} + \chi_{\perp}}, \quad \theta = \frac{2\chi_{\parallel}}{\chi_{\parallel} + \chi_{\perp}}. \quad (22)$$

Equations (17), (18), and (22) show that the thickness of the 180° CDWs is controlled by the longitudinal component of the dielectric susceptibility, while the 90° CDW thickness is controlled by the sum of the longitudinal and transverse susceptibilities. Also from Eq. (21), one sees that χ_{\perp} diverges as the MPB is approached. Such a divergence was first shown by Carl and Hardtl [19] and is corroborated with the enhanced piezoelectric properties of MPB materials. Thus the effect of anomalous 90° CDW thickness is associated with the divergence of the transverse dielectric susceptibility near the morphotropic boundary.

To analyze the polarization distribution in 90° CDW, we rewrite Eq. (12) in the form

$$P_y^2 + (1 - \theta)P_x^2 = (1 - \theta/2)P_0^2. \quad (23)$$

From this expression one obtains a mapping of the polarization profile on the plane $\{P_x, P_y\}$, which is an arc of an ellipse. One readily finds that as the MPB is approached ($\beta_2 - \beta_1 \rightarrow 0$), this arc converges to the arc of a circle, as illustrated in Fig. 2, line 1. Such order parameter trajectory is typical for ferromagnetic Néel walls but not for domain walls of proper ferroelectrics. Interestingly, order parameter behavior similar to that of ferroelectric Bloch walls was predicted in the improper ferroelectric $\text{Gd}_2(\text{MoO}_4)_3$ [20,21].

The reason for the unusual behavior of polarization in 90° ferroelectric CDWs is the ease of polarization rotation in proximity to the MPB. The Landau potential for polarization becomes nearly isotropic near the morphotropic boundary (within the approximation of expansion up to the fourth polarization power). Thus, from the point of view of the Landau potential, the trajectory of the CDW, where the polarization rotates with a constant modulus (Fig. 2, line 1), is optimal. The situation is, however, different in electrically neutral 90° DWs [Fig. 1(a)], where the polarization rotation is constrained by the depolarizing field and occurs with a simultaneous reduction of the polarization modulus. The polarization trajectory for an electrically neutral 90° DW is illustrated by line 2 in Fig. 2: In the first approximation, the polarization component normal to this wall remains constant, regardless of the Landau potential anisotropy (see, e.g., Ref. [5]). In contrast, in charged 90° domain walls, the electrostatic constraints are released due to the availability of free charge carriers. The free charges redistribute and screen the depolarizing field, enabling the polarization rotation.

The link between circular polarization mapping and large DW thickness may be explored as follows. In the frame of our model, the DW thickness is determined by a competition between two trends. The deviation of polarization from its spontaneous value in the DW region is penalized by a Landau energy excess. On one hand, to minimize this penalty, the DW tends to be narrower, and on the other hand, to minimize the effective correlation energy, the domain wall tends to be thicker. Near the MPB the Landau potential becomes isotropic and the Landau energy excess associated with the polarization rotation in 90° CDW tends to zero. Thus, the DW narrowing trend vanishes near MPB and, due to the thickening trend of the effective correlation energy, 90° CDWs become anomalously thick. The above analysis using a simple framework demonstrates the reasons for the thickening of the 90° charged domain walls near the morphotropic boundary. It is shown that this thickening effect is not expected in electrically neutral 90° DWs and in single-polarization-component 180° CDWs, making 90° CDWs unique in this sense. In the considered approximation, the thickness of the 90° CDW grows unlimitedly when approaching the MPB. However, in realistic systems, this growth is expected to be limited because of the anisotropy of the Landau potential, given by higher-order polarization powers, and because of constraints related to electromechanical coupling. To obtain a quantitative description of the effect of 90° CDW thickening near the MPB, we include these two factors in the model hereafter.

To describe the mechanical state of the domain wall, we use a standard procedure (see, e.g., Ref. [22]) where partially clamped conditions are applied, i.e., deformation components

$$u_{zz}(x) = u_{zz}|_{\infty}, \quad u_{yy}(x) = u_{yy}|_{\infty}, \quad u_{yz}(x) = u_{yz}|_{\infty}, \quad (24)$$

are fixed with the bulk values and stress components $\sigma_{xx} = \sigma_{xy} = \sigma_{xz} = 0$ are absent. Far from the wall, mechanically free boundary conditions are applied:

$$\sigma_{ij}(x \rightarrow \pm\infty) = 0, \quad i, j = 1, 2, 3. \quad (25)$$

Using this ansatz, the problem supplemented with mechanical degrees of freedom and with higher-order terms in polarization

in the free energy expansion is described by the following set of equations, which generalizes Eqs. (11) and (12):

$$\begin{aligned} &(\alpha - 2Q_{12}\sigma_{zz} - 2Q_{-}\sigma_{yy})P_x + \frac{\beta_1 + \beta_2}{2}P_x^3 \\ &+ \frac{(3\beta_1 - \beta_2)}{2}P_x P_y^2 + \frac{1}{4}P_x[P_x^4(\gamma_1 + 3\gamma_2) \\ &+ (2P_x^2 P_y^2 + P_y^4)(5\gamma_1 - \gamma_2)] + \left(\frac{\partial\rho}{\partial\varphi}\right)^{-1} \frac{d^2 P_x}{dx^2} = 0, \end{aligned} \quad (26)$$

$$\begin{aligned} &(\alpha - 2Q_{12}\sigma_{zz} - 2Q_{+}\sigma_{yy})P_y + \frac{\beta_1 + \beta_2}{2}P_y^3 \\ &+ \frac{(3\beta_1 - \beta_2)}{2}P_y P_x^2 + \frac{1}{4}P_y[P_y^4(\gamma_1 + 3\gamma_2) \\ &+ (2P_y^2 P_x^2 + P_x^4)(5\gamma_1 - \gamma_2)] = 0, \end{aligned} \quad (27)$$

$$s_{+}\sigma_{yy} + s_{12}\sigma_{zz} + 2Q_{-}P_x^2 + 2Q_{+}P_y^2 = \left(\frac{Q_{11} + Q_{12}}{2}\right)P_0^2, \quad (28)$$

$$s_{12}\sigma_{yy} + s_{11}\sigma_{zz} + 2Q_{12}(P_x^2 + P_y^2) = Q_{12}P_0^2, \quad (29)$$

$$Q_{\pm} = \frac{1}{2}(Q_{11} + Q_{12} \pm Q_{44}), \quad (30)$$

$$s_{\pm} = \frac{1}{2}\left(s_{11} + s_{12} + \frac{1}{2}s_{44}\right), \quad (31)$$

where Q_{11} , Q_{12} , and Q_{44} [23] are the components of electrostriction tensor in the crystallographic frame, s_{11} , s_{12} , and s_{44} are the corresponding components of the elastic compliance tensor, and γ_1 and γ_2 come from the expansion of the Landau potential $\Delta\Phi = \frac{\gamma_1}{6}(P_1^6 + P_2^6) + \frac{\gamma_2}{2}(P_1^4 P_2^2 + P_2^4 P_1^2)$. Voigt notations are used according to the reference text [24]. Here Eqs. (28) and (29) represent clamping conditions (24) for u_{yy} and u_{zz} , respectively. From the symmetry of the problem, $u_{yz} = \sigma_{yz} = 0$. Boundary conditions for the polarization vector, Eq. (8), are modified according to the rule

$$P_0 \rightarrow P_s = \sqrt{\frac{\sqrt{\beta_1^2 - 4\alpha\gamma_1} - \beta_1}{2\gamma_1}}.$$

The system of Eqs. (25)–(31) may be analytically reduced to the equation

$$\alpha^* P_x + \beta^* P_x^3 + \gamma^* P_x^5 \dots = -\left(\frac{\partial\rho}{\partial\varphi}\right)^{-1} \frac{d^2 P_x}{dx^2}, \quad (32)$$

where the coefficients of the series on the left-hand side (α^* , β^* , γ^* , etc.) are functions of the material properties enumerated above. For the 90° CDW half-width we use the approximation

$$\delta_{90}^{(ND^*)} = \left(\frac{9\sqrt{2}\pi^4 \hbar^6}{q^5 m^3 |\alpha^*|^3 P_s}\right)^{1/5}, \quad (33)$$

which is consistent with Eq. (20), within the substitution $\tilde{\alpha} \rightarrow \alpha^*$, $P_0 \rightarrow P_s$. An approximation for the DW thickness using only the first coefficient in the Landau series gives reasonable accuracy (about 10%) when $(\beta^*)^2 > \alpha^* \gamma^*$ (see, e.g., Ref. [2]), which is the case here.

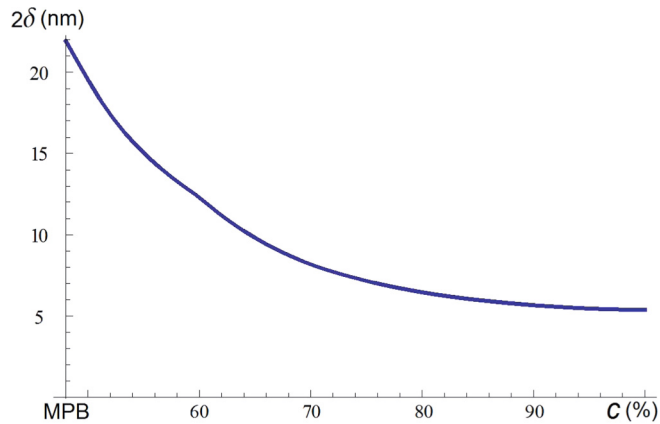


FIG. 3. (Color online) Charged 90° domain wall thickness in $\text{PbZr}_{1-c}\text{Ti}_c\text{O}_3$ at room temperature as a function of Ti content c , calculated numerically with the parameters given in Refs. [25,26].

Using Eq. (33), the 90° CDW thickness is calculated numerically for the parameters of $\text{Pb}(\text{Zr}_{1-c}\text{Ti}_c)\text{O}_3$ (PZT) of Refs. [25,26]. The dependence of the DW thickness on the Ti content (c) in PZT at room temperature is shown in Fig. 3. This figure demonstrates a fourfold DW thickness growth from 5.4 nm far from the MPB to 22 nm at the MPB. It is instructive to recall that the phase transition which determines the unique dielectric properties of MPB materials is not driven by temperature but by composition. Hence the large thickness of the 90° CDWs is predicted here for a wide temperature range. This fact is favorable for the robustness of electronic devices that may be potentially constructed using 90° CDWs.

The scenario described above for MPB materials may also be applied to BaTiO_3 in proximity to the transition from the tetragonal to the orthorhombic phase. In tetragonal BaTiO_3 one can expect thick 90° CDWs at room temperature, where a large dielectric susceptibility anisotropy $\chi_\perp/\chi_\parallel \simeq 30$ is observed due to the proximity to the orthorhombic phase [14]. The dependence of the DW thickness on the temperature, using the parameters of BaTiO_3 (given in Ref. [27]), is shown in Fig. 4. It is seen that the DW widening takes place on both sides of the tetragonal phase. Near the transition to the orthorhombic phase, the CDW thickness reaches 70 nm, which is about 2.5 times larger than in the middle of the tetragonal phase.

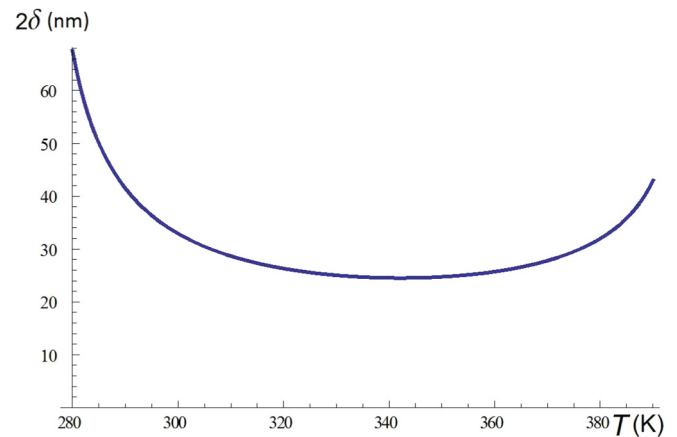


FIG. 4. (Color online) The dependence of charged 90° domain wall thickness in BaTiO_3 on temperature, calculated numerically using Eqs. (26)–(31) and material parameters from Ref. [27].

In summary, it was shown that, unlike neutral DWs and 180° CDWs, the free-carrier compensated 90° CDWs become substantially thicker near the MPB. The underlying mechanism is linked to an easy polarization rotation explained by the large anisotropy of dielectric susceptibility. Such an anisotropy is also observed in BaTiO_3 at room temperature, where 90° CDW thickening is predicted as well. In contrast to the case of BaTiO_3 , where the thickening is driven by a temperature change, in MPB materials the large thickness of the 90° CDW is predicted for a broad temperature interval. This property is favorable for potential electronic applications. The internal structure of the anomalously thick ferroelectric domain walls is analogical to Néel walls in ferromagnets. As in ferromagnets, the nature of the unique properties of 90° charged ferroelectric domain walls is related to the weak anisotropy of the Landau potential.

The research leading to these results has received funding from the European Research Council under the EU 7th Framework Programme (FP7/2007-2013)/ERC Grant Agreement No. 268058) and from the Swiss National Science Foundation (Grant No. 200020_140539/1). Additional support was received from the Section for Development and Cooperation of the Swiss Foreign Ministry (Agreement CH-3-SMm-01/02_2483 Swiss-Lithuania cooperation).

-
- [1] C. Kittel, *Introduction to Solid State Physics*, 4th ed. (Wiley, New York, 1971), Chap. 16.
- [2] A. K. Tagantsev, L. E. Cross, and J. Fousek, *Domains in Ferroic Crystals and Thin Films* (Springer, New York, 2010), Chap. 6.2.2, pp. 300–304.
- [3] S. Y. Yang, J. Seidel, S. J. Byrnes, P. Shafer, C. H. Yang, M. D. Rossell, P. Yu, Y. H. Chu, J. F. Scott, J. W. Ager, L. W. Martin, and R. Ramesh, *Nat. Nanotechnol.* **5**, 143 (2010).
- [4] J. Seidel, L. W. Martin, Q. He, Q. Zhan, Y. H. Chu, A. Rother, M. E. Hawkrigde, P. Maksymovych, P. Yu, M. Gajek, N. Balke, S. V. Kalinin, S. Gemming, F. Wang, G. Catalan, J. F. Scott, N. A. Spaldin, J. Orenstein, and R. Ramesh, *Nat. Mater.* **8**, 229 (2009).
- [5] P. Marton, I. Rychetsky, and J. Hlinka, *Phys. Rev. B* **81**, 144125 (2010).
- [6] P. Maksymovych, A. N. Morozovska, P. Yu, E. A. Eliseev, Y.-H. Chu, R. Ramesh, A. P. Baddorf, and S. V. Kalinin, *Nano Lett.* **12**, 209 (2012).
- [7] T. Sluka, A. Tagantsev, P. Bednyakov, and N. Setter, *Nat. Commun.* **4**, 1808 (2013).
- [8] B. M. Vul, G. M. Guro, and I. I. Ivanchik, *Ferroelectrics* **6**, 29 (1973).

- [9] M. Y. Gureev, A. K. Tagantsev, and N. Setter, *Phys. Rev. B* **83**, 184104 (2011).
- [10] V. D. Kugel and G. Rosenman, *Appl. Phys. Lett.* **62**, 2902 (1993).
- [11] M. Schroeder, A. Haussmann, A. Thiessen, E. Soergel, T. Woike, and L. M. Eng, *Adv. Funct. Mater.* **22**, 3936 (2012).
- [12] C.-L. Jia, S.-B. Mi, K. Urban, I. Vrejoiu, M. Alexe, and D. Hesse, *Nat. Mater.* **7**, 57 (2008).
- [13] T. Sluka, A. K. Tagantsev, D. Damjanovic, M. Gureev, and N. Setter, *Nat. Commun.* **3**, 748 (2012).
- [14] M. Zgonik, P. Bernasconi, M. Duelli, R. Schlessler, P. Gunter, M. H. Garrett, D. Rytz, Y. Zhu, and X. Wu, *Phys. Rev. B* **50**, 5941 (1994).
- [15] The 90° CDW may be head to head or tail to tail, i.e., with opposite charges, but with analogical properties. We consider here the head-to-head type. In the frame of our model, the results for a tail-to-tail CDW are the same within the substitution $\vec{P} \rightarrow -\vec{P}$ everywhere .
- [16] V. A. Zhirnov, *Sov. Phys.-JETP* **8**, 822 (1959).
- [17] The dielectric permittivity contribution is related to electrons and phonon modes other than the soft mode .
- [18] Note that, in general, the case $(\frac{\partial \rho}{\partial \varphi})^{-1}$ is a functional of $P(x)$ (Ref. [9]).
- [19] K. Carl and K. Hardtl, *Phys. Status Solidi A* **8**, 87 (1971).
- [20] A. Fouskova and J. Fousek, *Phys. Status Solidi A* **32**, 213 (1975).
- [21] B. D. Laikhtman and A. K. Tagantsev, *Fiz. Tverd. Tela* **17**, 1734 (1975) [*Sov. Phys. Solid State* **17**, 1127 (1975)].
- [22] A. K. Tagantsev, E. Courtens, and L. Arzel, *Phys. Rev. B* **64**, 224107 (2001).
- [23] $Q_{44} \equiv 2Q_{1212}$.
- [24] W. Martienssen, *Landolt-Bornstein: Numerical Data and Functional-Relationships in Science and Technology*, New Series Vol. III/16 and III/29a (Springer, Berlin, 1992).
- [25] M. J. Haun, E. Furman, S. Jang, and L. Cross, *Ferroelectrics* **99**, 45 (1989).
- [26] N. A. Pertsev, V. G. Kukhar, H. Kohlstedt, and R. Waser, *Phys. Rev. B* **67**, 054107 (2003).
- [27] J. Hlinka, P. Ondrejovic, and P. Marton, *Nanotechnology* **20**, 105709 (2009).